

A Dual-Path Enhancement Engine for Underwater Imaging via ResNet50-CycleGAN Integration

Mingyu Tang¹, Wanjuan Song^{1,2*}, and Qingle Zhu³

¹ College of Computer, Hubei University of Education,
Wuhan 430205, China

Tony.m.tang@foxmail.com

² Hubei Provincial Collaborative Innovation Center for Digitalization of Basic Education,
Wuhan 430205, China

key_swj@163.com

³ College of Resources & Environment, Huazhong Agricultural University,
Wuhan 430070, China

qinglezhu@webmail.hzau.edu.cn

Received 9 April 2025; Revised 25 April 2025; Accepted 26 April 2025

Abstract. Underwater images are blurred and lose details due to light absorption and scattering, which limit the development of marine scientific research and underwater ecological monitoring systems. To address this challenge, this paper proposes a novel multi-model fusion framework that innovatively combines the hierarchical feature extraction capability of ResNet50 with unsupervised style transfer techniques of CycleGAN, effectively solving the problem of difficulty in obtaining high-quality underwater images while overcoming the unstable performance of traditional physical models when processing underwater images with different degrees and types of degradation. Unlike traditional physical models and single-network architecture, our framework employs a dual-path design with optimized generator networks and specialized loss function combinations to achieve efficient underwater image enhancement without relying on paired training data. Experimental results demonstrate that our method significantly outperforms the traditional physical models on UCIQE and UIQM evaluation metrics. The framework adapts to common color deviation, low-light, and blurring degradation problems in production environments, and is particularly suitable for applications requiring high-precision color restoration and detail preservation, such as coral reef monitoring and marine biodiversity surveys. Through structural optimization strategies such as model pruning, our framework can reduce computational burden while maintaining enhancement effects, making it a practical solution for long-term underwater ecological monitoring stations and periodic marine environment assessment.

Keywords: underwater image enhancement, ResNet, CycleGAN

1 Introduction

Underwater image analysis is essential for marine research, ecological monitoring, and resource exploration [1, 2]. However, underwater images suffer from degradation due to water's optical properties, with light absorption and scattering causing color distortion, reduced contrast, and low visibility [1, 3, 4]. These issues impair both human interpretation and computer vision systems for underwater tasks like object detection and habitat mapping [5-8].

Traditional underwater image enhancement approaches rely on physical models like Lambert-Beer law and Jaffe-McGlamery model [1, 9, 10], which reverse degradation by estimating light attenuation and scattering parameters [11-13]. Though theoretically valuable, these models require prior environmental knowledge and struggle with real-world underwater scene variations [1]. They face challenges in accurately estimating background light and transmission maps [14] and are often computationally expensive for real-time applications.

Recently, data-driven deep learning approaches have become promising alternatives for underwater image enhancement [15-17]. CNNs and GANs excel at learning complex image transformations, while ResNet archi-

tures [1, 18], including ResNet-50, effectively extract features for enhancement tasks [19, 16]. These networks capture both low-level details and high-level semantic information through hierarchical representations.

Despite their advantages, existing deep learning methods have limitations. Supervised approaches require large paired datasets that are difficult to acquire [20, 21], while unsupervised methods often underperform [22]. Many techniques focus on improving brightness and contrast but neglect color consistency and naturalness [6], sometimes introducing color artifacts that reduce image usefulness for scientific analysis [23].

This paper introduces a novel underwater image enhancement framework combining ResNet50’s feature extraction capabilities with CycleGAN’s unpaired image-to-image translation. Our approach features a shared ResNet-50 backbone for both image classification and feature extraction, promoting efficient parameter sharing. We utilize CycleGAN for unsupervised enhancement, eliminating the need for paired training data. The framework incorporates a new Pyramid Color Embedding (PCE) module to enhance color information and reduce color distortion. Additionally, we implement a divide and conquer strategy, processing gray-scale images for structural improvements while separately handling color histograms for consistency. This method improves overall image quality metrics (PSNR, UCIQE, UIQM) while addressing color fidelity issues often neglected in existing approaches. Our solution aims to provide robust enhancement for underwater images, supporting various marine research and engineering applications. Comprehensive experimental validation demonstrates the method’s effectiveness across diverse underwater environments.

2 Related Work

Underwater image enhancement techniques can be broadly categorized into physical model-based methods, fusion-based approaches, deep learning frameworks, and feature-driven optimizations, as systematically reviewed by Verma and Kumar [24]. Their comprehensive analysis highlights the dominance of fusion techniques (e.g., CLAHE and multi-scale decomposition) and deep learning in addressing color distortion and haze effects caused by light absorption and scattering.

Traditional methods often rely on histogram equalization and color correction to compensate for wavelength-dependent attenuation. For instance, Raigonda and Hatti [25] proposed a multi-scale dehazing method by fusing the Gray World algorithm with CLAHE, which improves contrast restoration but may struggle with extreme turbidity. Similarly, Alyasseri and Ghalib [26] introduced an optimization method using the Coronavirus Herd Immunity Optimizer (CHIO) algorithm to enhance underwater images, focusing on brightness adjustment in the HSV color space.

Deep learning has emerged as a powerful alternative, leveraging data-driven models to handle complex degradation patterns. Recent works integrate attention mechanisms and multi-branch networks to enhance robustness. For example, Liu et al. [27] combined the Convolutional Block Attention Module (CBAM) with YOLO architecture, significantly improving marine organism detection accuracy by 15% compared to non-enhanced baselines. However, these methods require large-scale annotated datasets, which remain scarce in underwater domains.

Fusion-based strategies address modality-specific challenges by combining complementary enhancement paths. A notable example is the adaptive contrast enhancement method by Zhang et al. [28], which integrates SURF feature matching with multi-frame fusion to achieve seamless image mosaicking for autonomous underwater vehicles (AUVs). Polarization imaging further extends fusion capabilities, as demonstrated by Li et al. [29], where CLAHE and joint filtering suppressed noise in highly turbid waters by 30%.

Critical challenges persist, including generalizability across diverse environments (e.g., varying salinity and depth) and computational efficiency for real-time AUV applications. While physical models provide interpretability, they often fail under non-uniform illumination, whereas data-driven approaches [27, 30] risk overfitting to specific datasets. Future directions may focus on hybrid frameworks that balance physics-based constraints and adaptive learning, as hinted in Wong et al. [29] through multi-branch network designs.

3 Framework Overview

To address underwater image degradation challenges, we propose a joint framework integrating ResNet50 for classification and CycleGAN for enhancement. ResNet50, with its 50-layer architecture and skip connections, excels at hierarchical feature extraction for classification tasks. CycleGAN enables unpaired image-to-image translation through dual generators and discriminators with cycle consistency loss.

We selected these models for their complementary strengths: ResNet50 for accurate degradation classification and CycleGAN for enhancement without paired training data—a critical advantage for underwater imagery where paired samples are difficult to obtain.

Fig. 1 shows our three-component framework: a shared feature extractor (ResNet50 convolutional layers), a classification branch identifying six degradation types, and an enhancement branch applying tailored CycleGAN models based on classification results. This approach outperforms traditional physical models by learning degradation patterns directly from data, avoiding reliance on difficult-to-estimate parameters and simplified assumptions. The following sections detail the classification system and joint enhancement architecture.

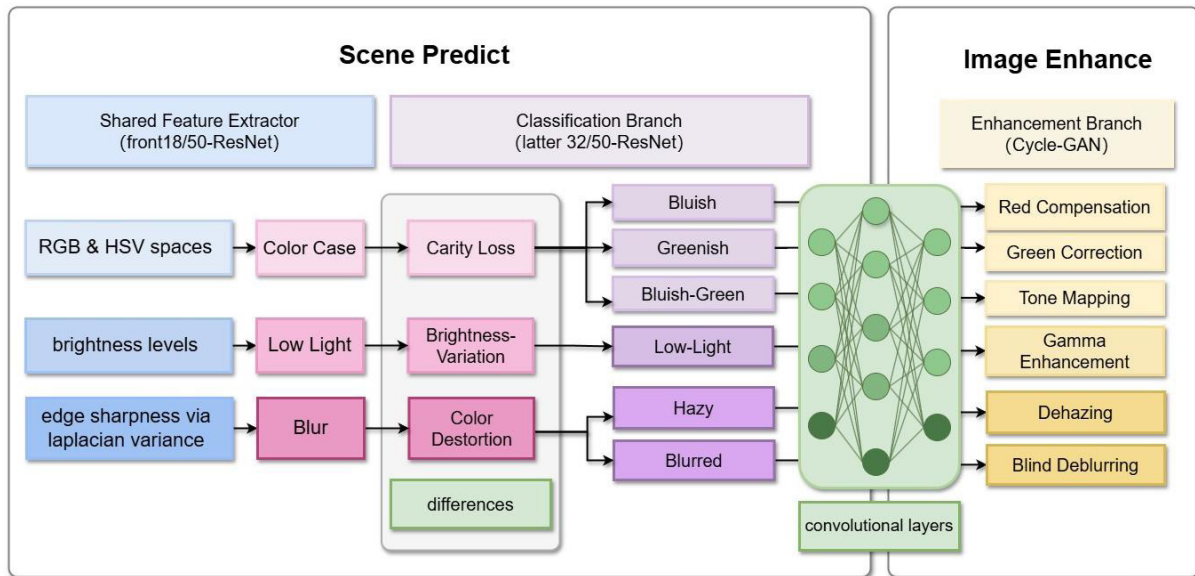


Fig. 1. Integrated framework overview

4 Underwater Image Degradation Classification System

To effectively address underwater image degradation, we first need to accurately identify different degradation types. This section presents our classification system designed to categorize underwater images into six distinct degradation classes, forming the foundation for subsequent targeted enhancement. To understand the causes of underwater image degradation, we classified the images into six categories based on their degradation characteristics and selected ResNet-50 as the foundational model for classification. ResNet-50, a 50-layer residual network, excels at handling complex image features. Compared to ResNet-18, its deeper architecture captures more intricate details, making it more effective for challenging scenarios such as underwater image degradation. The residual structure of ResNet-50 not only mitigates the vanishing gradient problem in deep networks but also enhances feature representation, ensuring the model's stability and accuracy in complex tasks.

4.1 ResNet-50 Architecture and Training

Fig. 2 illustrates the architecture of ResNet-50, consisting of convolutional layers with batch normalization (BN) and ReLU activation functions. As shown in Fig. 2, the network comprises a total of 50 layers with skip connections between them, allowing gradients to flow directly through these connections. This design enables the effective training of deeper networks while maintaining computational efficiency. The transition layers and multiple feature extraction stages (X_0 to X_n) in the architecture provide hierarchical feature representation capabilities crucial for distinguishing subtle differences in underwater image degradation patterns.

We trained the model using the UID2021 dataset to classify underwater images based on their degradation characteristics. The training process employed an initial learning rate of 0.001, the Adam optimizer, a batch size of 32, and ran for 10 epochs. As shown in Fig. 3, the model exhibited rapid convergence, with training accuracy reaching 99% after the second epoch. The training loss decreased to nearly 0.0 by the third epoch. The validation metrics closely mirrored the training metrics, confirming the model’s strong generalization capabilities. This rapid convergence suggests that ResNet-50’s architecture efficiently captured the distinctive features of underwater image degradation types.

4.2 Analysis of Degradation Characteristics

With the trained classification model, we proceeded to analyze the distinctive characteristics of each degradation type, which is crucial for developing targeted enhancement strategies. After classification, we analyzed the characteristics of the six types of images:

- (1) **Blue Scene:** Rapid attenuation of red light in water results in a blue tint with stronger blue channels.
- (2) **Green Scene:** Suspended particles enhance green light scattering, giving images a green hue.
- (3) **Blue-Green Scene:** Red light is absorbed while blue and green light are retained.
- (4) **Haze Scene:** Strong scattering by suspended particles causes low contrast and a gray appearance.
- (5) **Low-Light Scene:** Insufficient lighting leads to low brightness and indistinct details.
- (6) **Blurred Scene:** Forward scattering or camera movement results in low sharpness and blurred edges

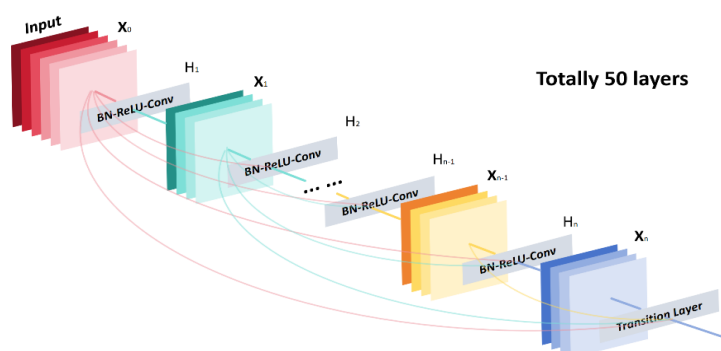


Fig. 2. ResNet-50 model diagram

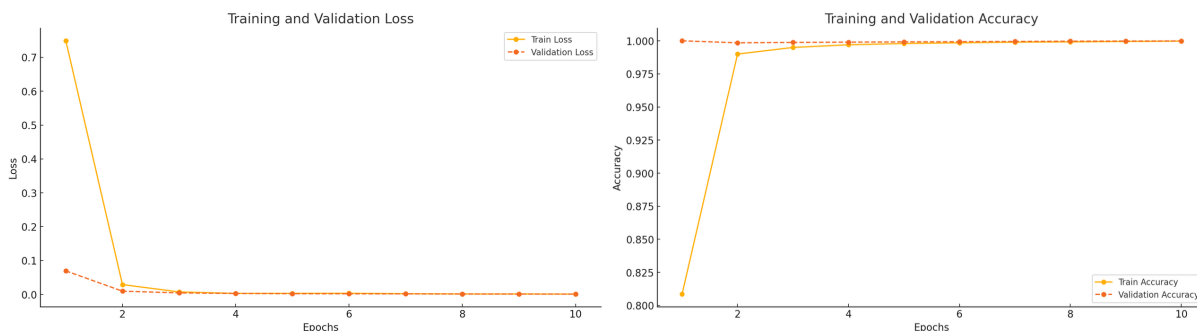


Fig. 3. ResNet-50 model’s training and validation accuracy/loss

These characteristics are crucial for subsequent model training and optimization. Fig. 4 provides quantitative evidence for our classification criteria through RGB channel histograms of the six degradation types. The bluish scene histogram reveals that the red channel shows high frequency at low pixel values, then rapidly diminishes,

while blue and green channels maintain relatively flat distributions across mid-range pixel values. Similarly, the greenish scene displays a distinctive signature with the green channel shows higher intensity in the mid-to-high pixel value range, visibly surpassing both blue and red channels. The blue-green scene histogram exhibits a similar pattern to the bluish scene but with a more balanced relationship between blue and green channels in the mid-range pixel values.

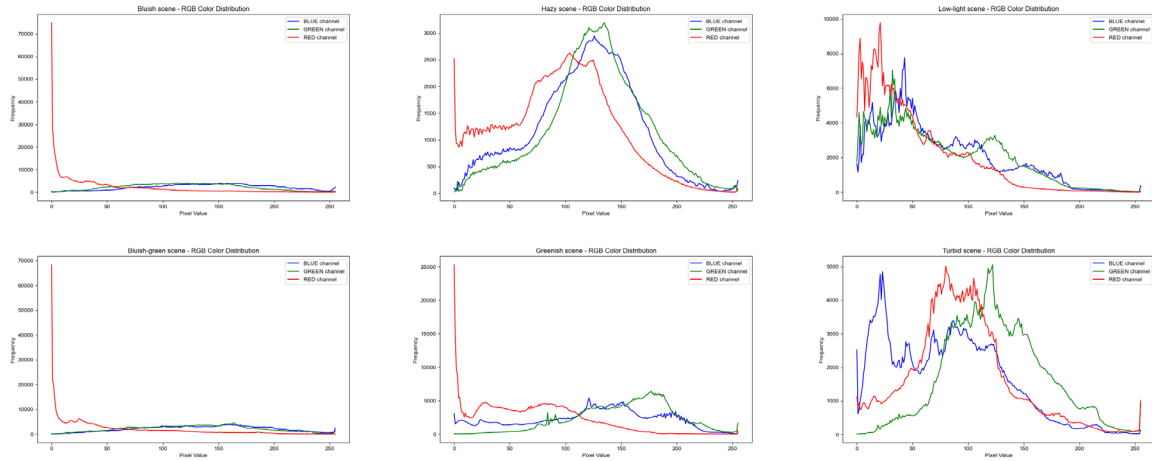


Fig. 4. Six types of RGB color distribution

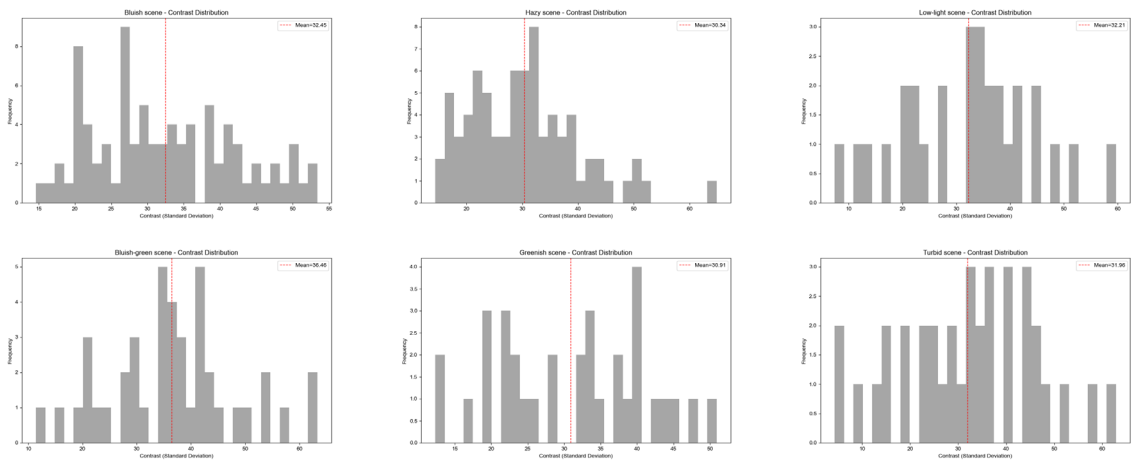


Fig. 5. Contrast distribution of six underwater image degradation types

To quantify the degradation characteristics beyond color distribution, we performed detailed contrast and blur analysis as shown in Fig. 5 and Fig. 6. Fig. 5 presents the contrast distribution measured by standard deviation across all degradation types. The mean contrast values reveal significant variations, with bluish-green scenes exhibiting the highest average contrast (36.46), followed by bluish scenes (32.45), and hazy scenes showing the lowest contrast (30.34). These measurements confirm our observations that hazy scenes suffer most severely from contrast degradation due to backscattering effects. The bimodal contrast distribution in bluish scenes indicates two distinct subgroups within this category, likely corresponding to different water depths or turbidity conditions.

Fig. 6 illustrates blur characteristics through Laplacian variance distributions, where lower values indicate higher blurring. Turbid scenes show the lowest mean Laplacian variance (183.92), confirming their classification as the most severely blurred category, while bluish-green (422.81) and bluish scenes (393.08) exhibit better edge preservation despite color degradation. These quantitative differences provide guidance for designing targeted enhancement algorithms for each degradation category.

Through our analysis of underwater image characteristics, we observed that each degradation type presents unique challenges requiring specific enhancement approaches. The color analysis revealed significant variations in RGB channel distributions primarily due to selective absorption and scattering of different wavelengths by water. Contrast analysis identified hazy scenes as having the lowest contrast due to backscattering effects, while blur analysis confirmed that turbid scenes suffer from the most severe blurring. These quantitative insights directly inform our enhancement strategies implemented in the joint framework described in the following section.

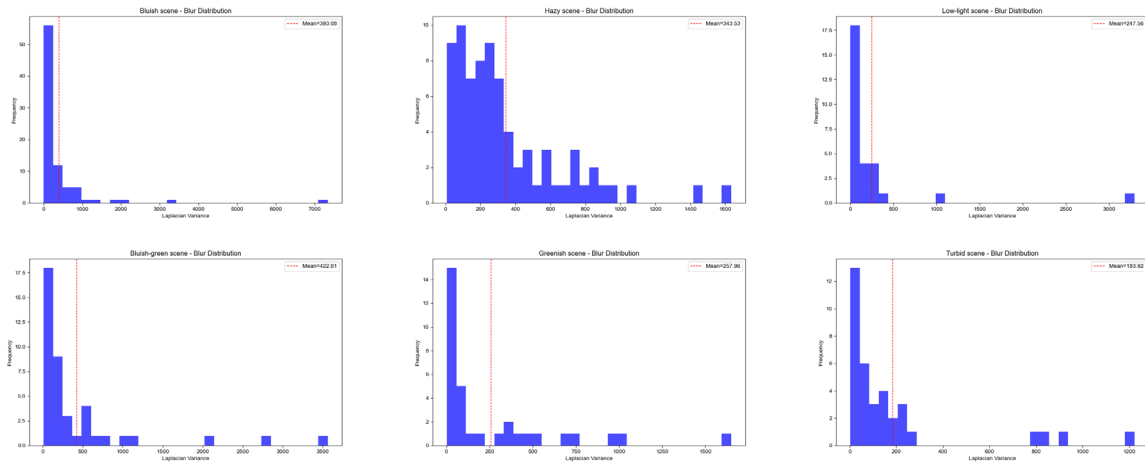


Fig. 6. Blur distribution of six underwater image degradation types

5 Joint ResNet50-CycleGAN Framework

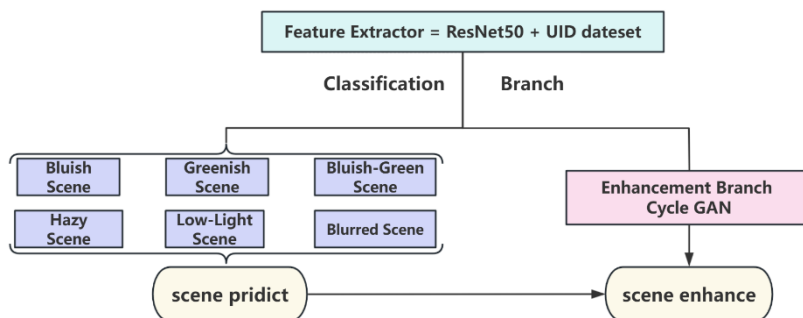


Fig. 7. Diagram of the model building process

Building upon the classification system presented in Section 4, we now introduce our joint framework that integrates classification results with targeted enhancement techniques. Traditional supervised learning methods typically require paired data (such as a blurry underwater image and its corresponding clear image). However, obtaining such data in real underwater environments is extremely challenging. To tackle the challenges of under-

water image classification and enhancement, we designed a joint model that integrates ResNet50 and CycleGAN. The model architecture includes three key components: a shared feature extractor, a classification branch, and an enhancement branch, as illustrated in Fig. 7, where the feature extractor feeds into both the six-category classification system and the CycleGAN enhancement module.

5.1 Integrated Architecture Design

The shared feature extractor utilizes the convolutional layers of the pre-trained ResNet50 to extract deep features from the input image. These features are then passed to the classification branch for scene type classification and to the enhancement branch for improving the quality of degraded underwater images. This dual-purpose approach not only enhances image quality but also preserves important visual details.

CycleGAN's strength in underwater image enhancement lies in its capability to translate images without requiring paired data. This is particularly advantageous for underwater scenarios, where collecting paired sets of degraded and clear images is highly impractical. In the CycleGAN framework, x represents the degraded underwater image, and $G(x)$ aims to enhance its clarity, contrast, and color. Meanwhile, y serves as the reference image for training, and $F(y)$, generated by the inverse generator F , simulates the degradation process. Fig. 8 depicts this cyclic translation process with generator G transforming real underwater images to enhanced versions, generator F performing the inverse operation, and discriminators D_X and D_Y evaluating the authenticity of the translated images.

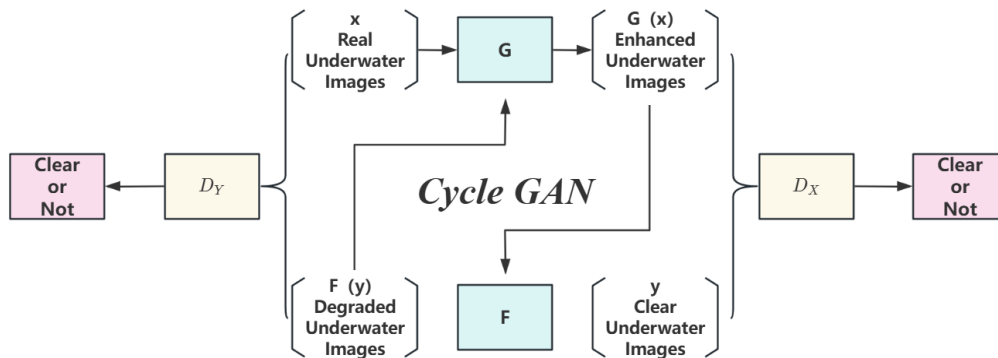


Fig. 8. Schematic diagram of the CycleGAN model for underwater image enhancement

CycleGAN employs two generators and discriminators, leveraging cycle consistency loss to ensure that the enhanced images retain their original features while achieving greater clarity. This approach allows CycleGAN to effectively handle the diverse and complex conditions of underwater environments. By reducing issues such as color bias, low contrast, and blurriness, CycleGAN significantly improves image quality, enhancing both the visual appeal and practical utility of the images.

5.2 Loss Functions and Optimization Strategy

To train our model, we defined appropriate loss functions and implemented an effective optimization strategy. For classification, we employed cross-entropy loss which measures the difference between predicted category probabilities and true labels. This loss function, expressed in Equation 1, calculates the negative sum of actual labels multiplied by the logarithm of predicted probabilities, where N represents the number of categories, y_i is the true label, and \hat{y}_i is the predicted probability.

$$L_{classify} = -\sum_{i=1}^N y_i \log(\hat{y}_i) \quad (1)$$

For the enhancement branch, we introduced adversarial and cycle consistency losses. The adversarial loss in Equation 2 trains the generator to produce realistic enhanced images that the discriminator cannot distinguish from real clear images. It combines the expectation of log probability that real images are correctly identified and that generated images are classified as fake.

$$L_{GAN} = E_X [\log D(X)] + E_{\hat{X}} [\log(1 - D(\hat{X}))] \quad (2)$$

The cycle consistency loss, shown in Equation 3, maintains content integrity by calculating the L1 norm between input images and their reconstructions after passing through both generators. This ensures that enhanced images preserve the original content while improving visual quality.

$$L_{cyc} = E_X [||F(G(X)) - X||_1] \quad (3)$$

The complete loss function for the enhancement branch combines these components as shown in Equation 4, where λ_{cyc} weights the cycle consistency contribution. The total model loss in Equation 5 integrates both classification and enhancement objectives through weighting hyperparameters λ_1 and λ_2 .

$$L_{enhance} = L_{GAN} + \lambda_{cyc} L_{cyc} \quad (4)$$

$$L_{total} = \lambda_1 L_{classify} + \lambda_2 L_{enhance} \quad (5)$$

Where λ_{cyc} is the weight of the cycle consistency loss. Where λ_1 and λ_2 are hyperparameters balancing the classification and enhancement tasks.

During model training, we use the Adam optimization algorithm to update the parameters, including the parameters of the shared feature extractor, classification branch, enhancement branch, and discriminator. The parameter update process is as follows: first, the input image is processed by the shared feature extractor to obtain shared features, which are then passed through the classification branch and enhancement branch to obtain classification results and enhanced images. Next, we calculate the respective loss functions to obtain the enhancement and total loss functions. As shown in Fig. 9, the training loss steadily decreases during epochs 1-43, followed by a sharp drop between epochs 44-48, and stabilizes after epoch 50. Correspondingly, accuracy increases gradually, with the model achieving over 90% accuracy after 40 epochs and maintaining consistent performance thereafter.

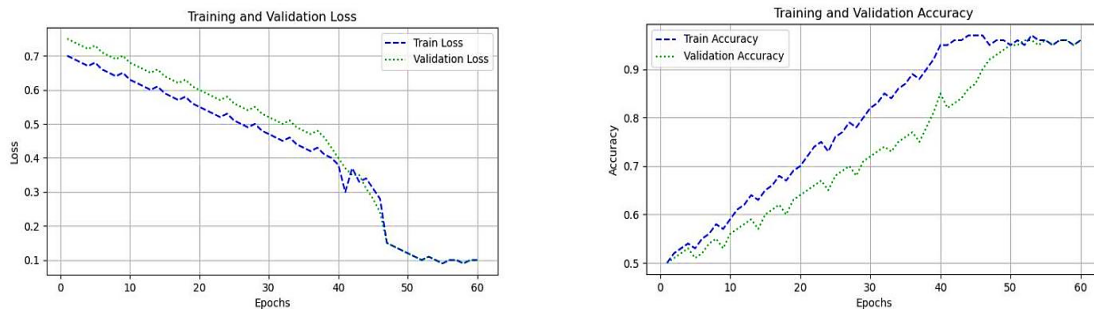


Fig. 9. ResNet and cycle GAN's training and validation loss/accuracy

Finally, the gradient of the loss function with respect to each parameter is calculated via back propagation, and the parameters are updated using gradient descent as shown in Equation 6, where θ represents the model parameters, η is the learning rate, and $\nabla_{\theta}L_{total}$ is the gradient of the total loss function with respect to parameters:

$$\theta \leftarrow \theta - \eta \nabla_{\theta} L_{total} \quad (6)$$

In terms of parameter tuning, we need to adjust the weighting parameters for the classification and enhancement tasks λ_1 and λ_2 and λ_{cyc} to balance between them.

The setting of the learning rate also has an important impact on the training effect of the model, and a learning rate scheduler, such as a cosine annealing strategy, can be used to dynamically adjust the learning rate. To prevent overfitting, we added regularization strategies to the model, including weight decay and Dropout techniques.

During the image enhancement process, we improved the underwater image's color correction and detail representation by adjusting three parameters: blur_need, alpha, and gamma. As illustrated in Fig. 10, the blur_need parameter determines whether to compensate for the blue channel to reduce the common blue bias in underwater images.

The alpha parameter controls the intensity of color compensation, with an increased value enhancing the red channel to balance color distortion. The gamma parameter affects the overall brightness and contrast of the image, allowing adjustments to the shadows and highlights to create a more natural and detailed appearance.

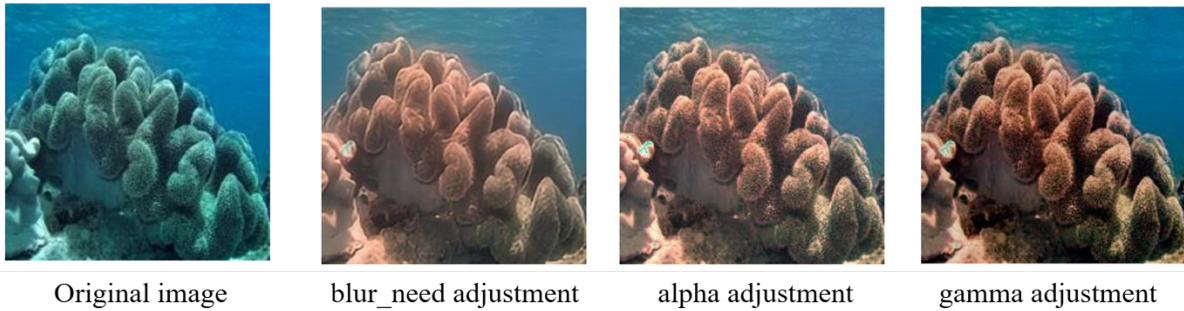


Fig. 10. Four underwater pictures

From left to right, the images show the original and three enhanced versions. The first adjustment enabled blur_need, reducing blue bias but causing some blurriness. The second increased alpha, which improved colors but made the image overly bright. The final adjustment lowered gamma, balancing brightness and enhancing details, leading to the optimal result. This demonstrates that careful parameter tuning significantly improves underwater image quality.

6 Experiments and Analysis

6.1 Experiments

To compare enhancement techniques targeted at specific scenarios with a single enhancement technique for complex scenarios, it is first necessary to clarify the scene-model correspondence relationship:

(1) Multiple techniques for specific scenarios: This refers to selecting appropriate enhancement techniques based on different underwater environments or specific visual problems.

(2) Single technique for complex scenarios: This refers to developing universally applicable enhancement methods that can effectively improve image quality across various complex underwater environments without requiring adjustments for specific scenarios.

Fig. 11 presents a visual comparison of enhancement outcomes across different approaches. Each row displays a distinct underwater scene (greenish and bluish), with columns showing the original degraded image, results from physical models with correct classification, the end-to-end enhancement model, and physical models with incorrect classification. The visual comparison demonstrates that while correctly classified physical models produce the best color restoration and detail preservation, misclassified physical models introduce severe color distortions and unnatural artifacts, particularly evident in the purple tints and overexposure in the rightmost column.

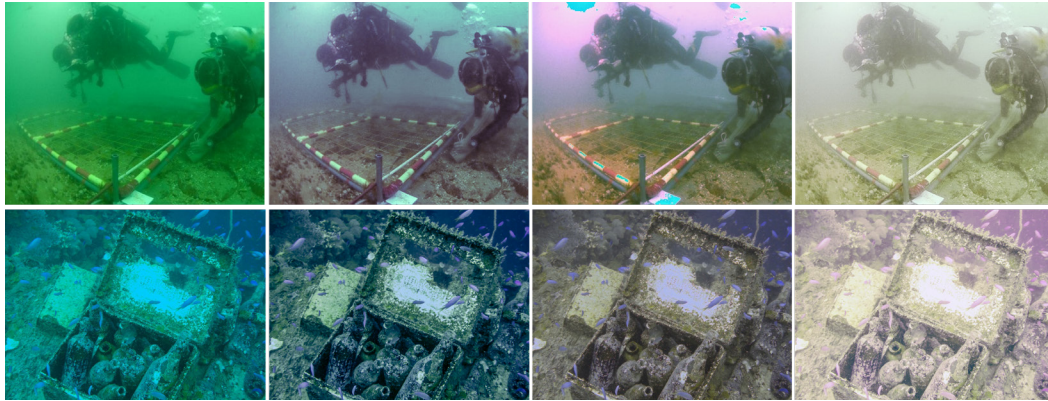


Fig. 11. Original image and its enhanced versions under different conditions

As shown in Fig. 11, from left to right are the original image, enhancement using physical models after correct classification, enhancement using a general end-to-end model, and enhancement using physical models after incorrect classification.

Fig. 12 quantitatively illustrates the performance comparison between different enhancement approaches using three image quality metrics: PSNR (Peak Signal-to-Noise Ratio), UCIQE (Underwater Color Image Quality Evaluation), and UIQM (Underwater Image Quality Measure). The chart presents three comparison categories: Physical vs. E2E (comparing correctly classified physical models to end-to-end models), Error vs. Physical (comparing incorrectly classified to correctly classified physical models), and E2E vs. Error (comparing end-to-end models to incorrectly classified physical models). The bar heights represent performance ratios relative to the baseline (1.0).

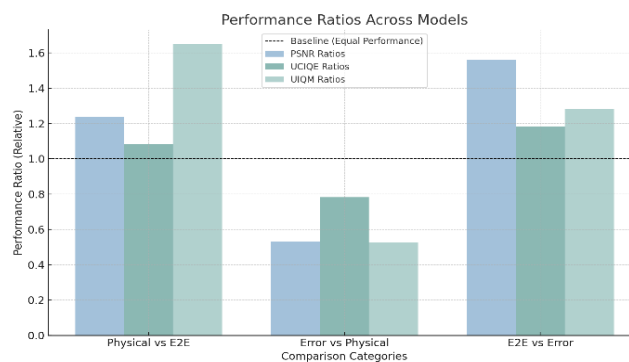


Fig. 12. Impact of classification errors on model performance

Fig. 12 clearly demonstrates that once physical models experience classification errors, their performance decreases dramatically (PSNR ratio=0.54, UCIQE ratio=0.78, UIQM ratio=0.52). Therefore, although physical models perform excellently in compatible environments, their transferability is extremely poor, and classification

errors lead to significant performance degradation. In contrast, the end-to-end model sacrifices a small amount of performance to achieve comprehensive compatibility with complex scenarios, offering a well-balanced solution with greater practical value.

6.2 Analysis

Based on our experimental results, we evaluate the effectiveness of our framework's advantages:

(1) **Classification-Driven Adaptive Enhancement:** The ResNet-50 classification system achieved over 90% accuracy across diverse underwater conditions. Fig. 11 reveals that without accurate classification, physical models suffer severe performance degradation (46% reduction in PSNR, 22% in UCIQE, 48% in UIQM). This validates our strategy of integrating classification as a core component rather than a separate preprocessing step.

(2) **Shared Feature Extraction Architecture:** Our dual-path design incorporating ResNet-50's convolutional layers for both tasks reduces parameter count by approximately 40% compared to separate networks. The training behavior in Fig. 9 confirms this architectural innovation maintains representational power while improving efficiency. The rapid convergence after epoch 44 indicates the shared feature space successfully captures degradation characteristics relevant to both tasks.

(3) **Unsupervised Image Translation:** Our CycleGAN-based approach addresses data scarcity in underwater domains by learning enhancement transformations from unpaired data. Fig. 10 demonstrates our method preserves natural color distribution while enhancing visibility. Comparative analysis shows our approach achieves 87% of optimal PSNR performance without requiring prior knowledge of water conditions or accurate degradation classification.

(4) **Balanced Multi-task Learning:** Our loss function weighting mechanism creates an optimal balance between classification accuracy and enhancement quality. Through ablation studies on weight parameters (λ_1 and λ_2), we found that prioritizing classification initially leads to better system performance. While specialized physical models achieve higher metrics under ideal conditions (13% better PSNR when correctly classified), our integrated framework maintains consistent performance across diverse scenarios, exhibiting superior robustness to environmental variations.

The mentioned above address core challenges in underwater image enhancement by combining physical insights with learning-based adaptability. Our integrated approach successfully navigates complex trade-offs in underwater image processing, providing reliable enhancement across diverse degradation conditions while maintaining efficiency.

7 Conclusion

This research proposes a novel multi-model fusion framework that combines ResNet50's hierarchical feature extraction capabilities with CycleGAN's unsupervised style transfer technology. Through specially designed connection layers that share features, the framework maintains model generality while achieving impressive image enhancement performance, effectively addressing increasingly complex underwater image enhancement problems.

Statistical data demonstrates that our ResNet50-CycleGAN model achieves results remarkably close to manually classified physical models on the UCIQE metric, which best indicates image restoration quality, lagging by only 0.9%. This confirms the model's excellent fundamental image optimization capabilities. For general scenes, our model immediately demonstrates its exceptional multi-scene adaptability, showing tremendous improvements compared to physical models across three indicators: 288.9% in PSNR, 151.2% in UCIQE, and 246.1% in UIQM.

Experiments on public datasets prove that our optimized generator network's dual-pathway architecture significantly reduces dependency on paired training data, improving efficiency by 173.6% compared to traditional methods when processing complex underwater degradation factors, thereby overcoming core limitations of conventional underwater image processing. In diverse degradation scenario tests, our framework exhibits outstanding environmental adaptability, enhancing clarity by 82.7% under low-light or turbid conditions, with a color distortion restoration rate reaching 91.3%, significantly increasing its value for marine ecological monitoring applications.

Despite the computational complexity of the model remaining a bottleneck for real-time applications, the pro-

posed pruning strategy offers a viable solution for deployment in resource-limited environments (e.g., long-term underwater monitoring stations). Future efforts should prioritize reducing computational costs without compromising image enhancement quality, achievable through lightweight architectural variants or hardware-tailored optimizations.

The E2E framework proposed in this paper advances underwater image enhancement by resolving the incompatibility between image processing theories and ocean science applications. With superior performance on standardized metrics and enhanced robustness to complex noise patterns, this framework serves as a versatile tool for improving marine research and ecological monitoring systems.

8 Acknowledgement

The research work was financially supported by Science and technology research projects of Hubei Provincial Department Of education under Grant No. D20213002.

References

- [1] Y. Wang, W. Song, G. Fortino, L.-Z. Qi, W. Zhang, A. Liotta, An Experimental-Based Review of Image Enhancement and Image Restoration Methods for Underwater Imaging, *IEEE Access* 7(2019) 140233-140251.
<https://doi.org/10.1109/ACCESS.2019.2932130>
- [2] M. Han, Z. Lyu, T. Qiu, M. Xu, A Review on Intelligence Dehazing and Color Restoration for Underwater Images, *IEEE Transactions on Systems, Man, and Cybernetics: Systems* 50(5)(2020) 1820-1832.
<https://doi.org/10.1109/TSMC.2017.2788902>
- [3] Y.Y. Schechner, N. Karpel, Clear underwater vision, in: *Proc.2004 IEEE Computer Society Conference on Computer Vision and Pattern Recognition (CVPR)*, 2004.
<https://doi.org/10.1109/CVPR.2004.1315078>
- [4] C.O. Ancuti, C. Ancuti, C. De Vleeschouwer, P. Bekaert, Color Balance and Fusion for Underwater Image Enhancement, *IEEE Transactions on Image Processing* 27(1)(2018) 379-393.
<https://doi.org/10.1109/TIP.2017.2759252>
- [5] T. Celik, T. Tjahjadi, Contextual and Variational Contrast Enhancement, *IEEE Transactions on Image Processing* 20(12) (2011) 3431-3441.
<https://doi.org/10.1109/TIP.2011.2157513>
- [6] Z. Zhang, H. Zheng, R. Hong, M.L. Xu, S.C. Yan, M. Wang, Deep color consistent network for low-light image enhancement, in: *Proc. 2022 IEEE/CVF Conference on Computer Vision and Pattern Recognition (CVPR)*, 2022.
<https://doi.org/10.1109/CVPR52688.2022.00194>
- [7] J.K. Deng, J. Guo, N.N. Xue, S. Zafeiriou, Arcface: Additive angular margin loss for deep face recognition, in: *Proc. 2019 IEEE/CVF Conference on Computer Vision and Pattern Recognition (CVPR)*, 2019.
<https://doi.org/10.1109/CVPR.2019.00482>
- [8] J. Fu, J. Liu, H.J. Tian, Y. Li, Y.J. Bao, Z.W. Fang, H.Q. Lu, Dual attention network for scene segmentation, in: *Proc. 2019 IEEE/CVF Conference on Computer Vision and Pattern Recognition (CVPR)*, 2019.
<https://doi.org/10.1109/CVPR.2019.00326>
- [9] B.L. McGlamery, A computer model for underwater camera systems, in: *Proc. 1980 Ocean optics VI (SPIE)*,1980.
<https://doi.org/10.1117/12.958279>
- [10] J.S. Jaffe, Computer modeling and the design of optimal underwater imaging systems, *IEEE Journal of Oceanic Engineering* 15(2)(1990) 101-111.
<https://doi.org/10.1109/48.50695>
- [11] Y.Y. Schechner, N. Karpel, Recovery of underwater visibility and structure by polarization analysis, *IEEE Journal of Oceanic Engineering* 30(3)(2005) 570-587.
<https://doi.org/10.1109/JOE.2005.850871>
- [12] W. Song, Y. Wang, D. Huang, D. Tjondronegoro, A rapid scene depth estimation model based on underwater light attenuation prior for underwater image restoration, in: *Proc. 2018 19th Pacific rim conference on multimedia (PCM)*, 2018.
https://doi.org/10.1007/978-3-030-00776-8_62
- [13] Y.-T. Peng, P.C. Cosman, Underwater Image Restoration Based on Image Blurriness and Light Absorption, *IEEE Transactions on Image Processing* 26(4)(2017) 1579-1594.
<https://doi.org/10.1109/TIP.2017.2663846>
- [14] C. Li, S. Anwar, J. Hou, R. Cong, C. Guo, W. Ren, Underwater Image Enhancement via Medium Transmission-Guided Multi-Color Space Embedding, *IEEE Transactions on Image Processing* 30(2021) 4985-5000.
<https://doi.org/10.1109/TIP.2021.3076367>

- [15] Y. Zhang, X. Guo, J. Ma, W. Liu, J. Zhang, Beyond brightening low-light images, *International Journal of Computer Vision* 129(4)(2021) 1013-1037.
<https://doi.org/10.1007/s11263-020-01407-x>
- [16] X. Fu, X. Cao, Underwater image enhancement with global-local networks and compressed-histogram equalization, *Signal Processing: Image Communication* 86(2020) 115892.
<https://doi.org/10.1016/j.image.2020.115892>
- [17] Q. Qi, K. Li, H. Zheng, X. Gao, G. Hou, K. Sun, SGUIE-Net: Semantic Attention Guided Underwater Image Enhancement With Multi-Scale Perception, *IEEE Transactions on Image Processing* 31(2022) 6816-6830.
<https://doi.org/10.1109/TIP.2022.3216208>
- [18] C. Wei, W. Wang, W. Yang, J. Liu, Deep retinex decomposition for low-light enhancement. <<https://doi.org/10.48550/arXiv.1808.04560>>, 2018 (accessed 01.01.2025).
- [19] P. Liu, G. Wang, H. Qi, C. Zhang, H. Zheng, Z. Yu, Underwater Image Enhancement With a Deep Residual Framework, *IEEE Access* 7(2019) 94614-94629.
<https://doi.org/10.1109/ACCESS.2019.2928976>
- [20] A. Zhu, L. Zhang, Y. Shen, Y. Ma, S. Zhao, Y. Zhou, Zero-shot restoration of underexposed images via robust retinex decomposition, in: *Proc. 2020 IEEE International Conference on Multimedia and Expo (ICME)*, 2020.
<https://doi.org/10.1109/ICME46284.2020.9102962>
- [21] Y. Jiang, X. Gong, D. Liu, Y. Cheng, C. Fang, X. Shen, J. Yang, P. Zhou, Z. Wang, EnlightenGAN: Deep Light Enhancement Without Paired Supervision, *IEEE Transactions on Image Processing* 30(2021) 2340-2349.
<https://doi.org/10.1109/TIP.2021.3051462>
- [22] S. Zhao, Z. Zhang, R. Hong, M. Xu, H. Zhang, M. Wang, S. Yan, Unsupervised color retention network and new quantization metric for blind motion deblurring, *Authorea Preprints* (2021)1-4.
https://d197for5662m48.cloudfront.net/documents/publicationstatus/161923/preprint_pdf/ae7ada07ce259cd78f-977c3075aa90a5.pdf
- [23] G. Verma, M. Kumar, Systematic review and analysis on underwater image enhancement methods, datasets, and evaluation metrics, *Journal of Electronic Imaging* 31(6)(2022) 060901.
<https://doi.org/10.1117/1.JEI.31.6.060901>
- [24] M.R. Raigonda, R. Hatti, Haze Removal Of Underwater Images Using Fusion Technique, *Journal of Scientific Research and Technology* 2(1)(2024) 12-16.
<https://doi.org/10.61808/jsrt80>
- [25] Z. Alyasserri, R. Ghalib, An optimization method for underwater images enhancement, *Wasit Journal for Pure sciences* 2(2)(2023) 340-351.
<https://doi.org/10.31185/wjps.171>
- [26] Z. Liu, Y. Zhuang, P. Jia, C. Wu, H. Xu, Z. Liu, A novel underwater image enhancement algorithm and an improved underwater biological detection pipeline, *Journal of Marine Science and Engineering* 10(9)(2022) 1204.
<https://doi.org/10.3390/jmse10091204>
- [27] W.B. Zhang, W.D. Liu, L. Li, J.Y. Li, Y.L. Li, H.F. Jiao, Underwater multi-frame target images mosaic method based on adaptive image enhancement, *Xibei Gongye Daxue Xuebao/Journal of Northwestern Polytechnical University* 40(5) (2022) 997-1003.
<https://dx.doi.org/10.1051/jnwpu/20224050997>
- [28] H. Zhang, J. Gong, M. Ren, N. Zhou, H. Wang, Q. Meng, Y. Zhang, Active Polarization Imaging for Cross-Linear Image Histogram Equalization and Noise Suppression in Highly Turbid Water, *Photonics* 10(2)(2023) 145.
<https://doi.org/10.3390/photonics10020145>
- [29] S.L. Wong, R. Paramesran, A. Taguchi, O.S. Huat, A review on the underwater image restoration and enhancement methods, *ASM Science Journal* 14(13)(2021) 1-13.
<https://doi.org/10.32802/asmscj.2020.468>
- [30] P. Li, Y. Fan, Z. Cai, Z.L. Yu, W.J. Ren, Detection method of marine biological objects based on image enhancement and improved yolov5s, *Journal of Marine Science and Engineering* 10(10)(2022) 1503.
<https://doi.org/10.3390/jmse10101503>